

RESEARCH ARTICLE

# Physiologically driven, altitude-adaptive model for the interpretation of pediatric oxygen saturation at altitudes above 2,000 m a.s.l.

Laura Tüshaus,<sup>1\*</sup> Monica Moreo,<sup>1\*</sup> Jia Zhang,<sup>1</sup> Stella Maria Hartinger,<sup>2,3,4</sup> Daniel Mäusezahl,<sup>3,4</sup> and  Walter Karlen<sup>1</sup>

<sup>1</sup>Mobile Health Systems Lab, Institute for Robotics and Intelligent Systems, Department of Health Sciences and Technology, ETH Zurich, Switzerland; <sup>2</sup>Universidad Peruana Cayetano Heredia, Lima, Peru; <sup>3</sup>Department of Epidemiology & Public Health, Swiss Tropical and Public Health Institute (Swiss TPH), Basel, Switzerland; and <sup>4</sup>University of Basel, Basel, Switzerland

Submitted 31 May 2018; accepted in final form 24 June 2019

**Tüshaus L, Moreo M, Zhang J, Hartinger SM, Mäusezahl D, Karlen W.** Physiologically driven, altitude-adaptive model for the interpretation of pediatric oxygen saturation at altitudes above 2,000 m a.s.l. *J Appl Physiol* 127: 847–857, 2019. First published August 8, 2019; doi:10.1152/jappphysiol.00478.2018.—Measuring peripheral oxygen saturation (SpO<sub>2</sub>) with pulse oximeters at the point of care is widely established. However, since SpO<sub>2</sub> is dependent on ambient atmospheric pressure, the distribution of SpO<sub>2</sub> values in populations living above 2000 m a.s.l. is largely unknown. Here, we propose and evaluate a computer model to predict SpO<sub>2</sub> values for pediatric permanent residents living between 0 and 4,000 m a.s.l. Based on a sensitivity analysis of oxygen transport parameters, we created an altitude-adaptive SpO<sub>2</sub> model that takes physiological adaptation of permanent residents into account. From this model, we derived an altitude-adaptive abnormal SpO<sub>2</sub> threshold using patient parameters from literature. We compared the obtained model and threshold against a previously proposed threshold derived statistically from data and two empirical data sets independently recorded from Peruvian children living at altitudes up to 4,100 m a.s.l. Our model followed the trends of empirical data, with the empirical data having a narrower healthy SpO<sub>2</sub> range below 2,000 m a.s.l. but the medians never differed more than 2.3% across all altitudes. Our threshold estimated abnormal SpO<sub>2</sub> in only 17 out of 5,981 (0.3%) healthy recordings, whereas the statistical threshold returned 95 (1.6%) recordings outside the healthy range. The strength of our parametrized model is that it is rooted in physiology-derived equations and enables customization. Furthermore, as it provides a reference SpO<sub>2</sub>, it could assist practitioners in interpreting SpO<sub>2</sub> values for diagnosis, prognosis, and oxygen administration at higher altitudes.

**NEW & NOTEWORTHY** Our model describes the altitude-dependent decrease of SpO<sub>2</sub> in healthy pediatric residents based on physiological equations and can be adapted based on measureable clinical parameters. The proposed altitude-specific abnormal SpO<sub>2</sub> threshold might be more appropriate than rigid guidelines for administering oxygen that currently are only available for patients at sea level. We see this as a starting point to discuss and adapt oxygen administration guidelines.

altitude; child health; hypoxemia; model; oxygen saturation; physiological adaptation; pneumonia

## INTRODUCTION

Acute lower respiratory infections (ALRI) are a major health burden in low- and middle-income countries. Childhood pneumonia accounts for 14% of all deaths in children worldwide under 5 years of age (45), of which 95% occur in low resource settings (41). Common conditions observed in ALRI are dyspnea and hypoxemia, an abnormally low level of oxygen saturation in the arterial blood (SaO<sub>2</sub>) that can lead to cyanosis and subsequently to death (43). A rapid and noninvasive estimation of hypoxemia can be obtained through pulse oximetry that measures peripheral oxygen saturation (SpO<sub>2</sub>). Pulse oximetry has become a suitable technology for application in low resource settings due to the simplicity of use in combination with mobile phones and noninvasiveness of the device (20, 27). The use of pulse oximeters and supplemental oxygen in clinical applications at the point of care has shown to drastically reduce death rates (8). However, in countries where these devices are needed most, health personnel have only slowly started to gain access.

The interpretation of SpO<sub>2</sub> values for hypoxemia is challenging, especially for health personnel not familiar with respiratory physiology and measurement principles of pulse oximeters. The World Health Organization (WHO) recommends the administration of oxygen when SpO<sub>2</sub> drops below or is equal to 90% (44). This fixed threshold oversimplifies hypoxemia treatment (7). It does not provide an indication on when to stop treatment and does not permit adaptation to the local conditions. Namely, in many rural areas, oxygen is a scarce and precious resource and therefore only restrictively administered. Altitude has a direct influence on SpO<sub>2</sub> as the air pressure decreases and, consequently, the alveolar oxygen partial pressure decreases with increasing altitude (43). Thus, the treatment of ALRI (i.e., administration of oxygen), diagnosis, and prognosis might be affected at higher altitudes and the recommended oxygen administration guidelines at sea level may not be applicable. However, before determining treatment thresholds at higher altitudes, healthy values in this environment need to be established.

\* L. Tüshaus and M. Moreo contributed equally to this work.

Address for reprint requests and other correspondence: W. Karlen, ETH Zurich, Mobile Health Systems Lab, Institute of Robotics and Intelligent Systems, Dept. of Health Sciences and Technology, BAA, Lengghalde 5, 8092 Zurich, Switzerland (e-mail: walter.karlen@ieee.org).

In this work, we introduce an altitude-adaptive SpO<sub>2</sub> model and propose a model-derived altitude-adaptive abnormal SpO<sub>2</sub> threshold. The physiology-backed altitude-adaptive model describes SpO<sub>2</sub> values of healthy children living permanently at altitudes up to 4,000 m a.s.l. With this model, we aim to provide a better understanding of healthy SpO<sub>2</sub> values at altitudes above 2,000 m a.s.l. for healthy children. The altitude-adaptive abnormal SpO<sub>2</sub> threshold is obtained by setting the model parameters to abnormal values found in hypoxemic patients. We evaluate these results with a novel data set obtained from healthy children living in the rural Andes of Peru.

### Related Work

The current literature presents two modeling approaches that describe the relationship between SpO<sub>2</sub> and altitude.

Subhi et al. (40) developed a statistical model of the SpO<sub>2</sub> distribution across altitudes that is based on empirical observations from healthy children and derived an altitude-adaptive threshold for hypoxemia from this model. Data were obtained through a literature review of studies performed between 0 and 4,018 m a.s.l. A linear random effects meta-regression was performed to predict mean and 2.5th centile SpO<sub>2</sub> with an exponential equation. This 2.5th centile of healthy children's SpO<sub>2</sub> at each altitude was proposed as an altitude-adjusted hypoxemia threshold. It is unclear why this specific, statistically derived threshold was chosen. The obtained statistical model and threshold also did not take other influencing factors, such as measurement protocols, choice of oximeter technology, ethnicity, and age range of the studied subjects, into account.

Our group developed a computer model that described the pathway of oxygen throughout the cardiorespiratory body compartments (24, 25). It implemented the oxygen cascade described by West (43). The model used well established physiological equations to explain how the partial oxygen pressure and oxygen concentrations are interrelated between alveolar gas and peripheral blood (24) (Fig. 1). The oxygen cascade describes the oxygen loss from the partial pressure of

inspired air to the resulting measurements of SpO<sub>2</sub> by a pulse oximeter. Therefore, the model was based on physiological parameters and integrated pulse oximeter measurement inaccuracies as reported by the manufacturer. A shortcoming of the model was that it assumed many physiological parameters to be constant and therefore did not consider altitude adaptation. Consequently, it could not correctly describe SpO<sub>2</sub> measured at higher altitudes, especially in people adapted to these conditions, such as permanent residents.

In a recent prospective study, Rojas-Camayo et al. recorded SpO<sub>2</sub> from 6,289 subjects ranging from infants to elderly people in the Peruvian Andes at 15 altitudes from 154 m to 5,100 m a.s.l (36). They reported the 2.5th, 10th, 25th, 50th, 75th, 90th and 97.5th centile of the empirical data. This data has not been used to derive a hypoxemia threshold thus far.

### MODELING

#### Altitude-Adaptive SpO<sub>2</sub> Model

Starting from the previously established computer model of the oxygen cascade (24), we modified this model to include physiological adaptation to high altitudes. We adjusted parameters that had been found to change with altitude in permanent residents (see Table 1 for an overview of all parameters used). Briefly, the existing model of the oxygen cascade described the pathway of oxygen throughout the cardiorespiratory body compartments (Fig. 1) using physiological equations (see APPENDIX). The model was originally developed to estimate the "virtual shunt" (VS) describing the overall loss of oxygen content between the alveolar gas and arterial blood compartments (2), with SpO<sub>2</sub> and inspired oxygen (FiO<sub>2</sub>) values as input parameters. An increase in the VS is one of the main causes of hypoxemia (43).

The above mentioned oxygen cascade model, originally developed for adults, can be adapted to a pediatric model as there are no indications that the underlying physics of gas exchange are any different in children (28). We identified relationships between altitude adaptation and parameters of the oxygen cascade, such as atmospheric pressure, hemoglobin

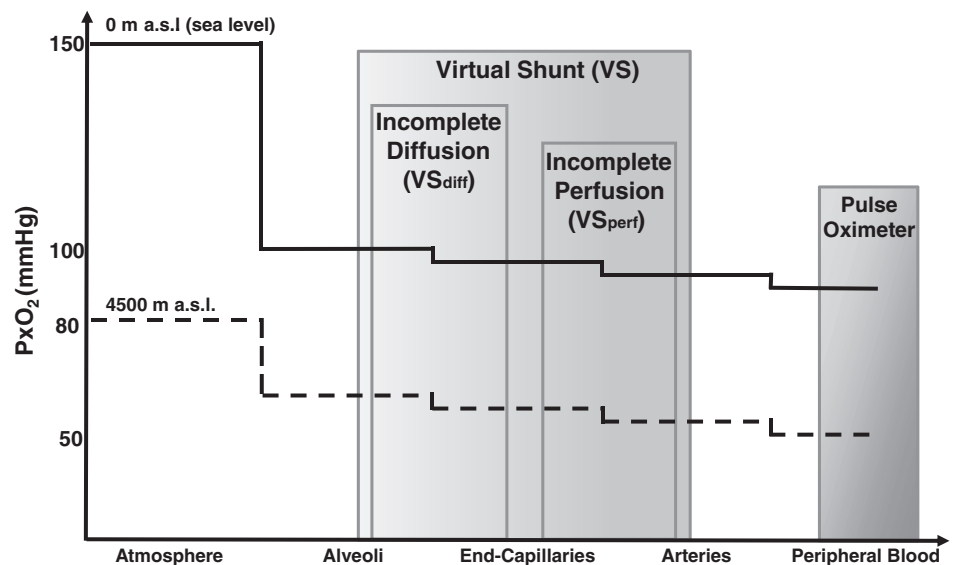


Fig. 1. Oxygen cascade describing the loss in oxygen partial pressure (PO<sub>2</sub>) between inspired air and peripheral blood measured with a pulse oximeter. Lines illustrate the standard situation for a healthy subject at sea level (continuous) and at 4,500 m a.s.l. (dashed). Virtual shunt (VS) describes the combined loss in oxygen content due to incomplete diffusion (VS<sub>diff</sub>) or perfusion (VS<sub>perf</sub>) between alveolar and arterial compartments.

Table 1. *Physiological parameters obtained from the literature used to implement the altitude-adaptive SpO<sub>2</sub> model*

| Parameter                    | Unit     | Ref.         | Healthy Ranges   |      |      |                |      |      | Hypoxemia                            |
|------------------------------|----------|--------------|--|------|------|----------------|------|------|--------------------------------------|
|                              |          |              | Sea level  |      |      | 4,500 m a.s.l. |      |      |                                      |
|                              |          |              | Min  | mean | max  | min            | mean | max  |                                      |
| P <sub>ACO<sub>2</sub></sub> | mmHg     | (30, 32, 35) | 35   | 40   | 45   | 23             | 28.3 | 33   | Assumed to be equal to healthy range |
| RQ                           | unitless | (32, 43)     | 0.8  | 0.8  | 1    | 1              | 1    | 1    |                                      |
| cHb                          | g/100 ml | (43)         | 12   | 15   | 17.5 | 17             | 20   | 22.5 | ≥5*                                  |
| VS <sub>perf</sub>           | %        | (31)         | 0  | 2    | 5    | 0              | 2    | 5    |                                      |
| VS <sub>diff</sub>           | %        | Derived      | 0  | 0    | 0    | 0              | 0    | 0    | ≥19*                                 |
| PAO <sub>2</sub>             | mmHg     | Derived      | Derived by the alveolar gas equation, with parameters FiO <sub>2</sub> , P <sub>atm</sub> , PH <sub>2</sub> O, P <sub>ACO<sub>2</sub></sub> and RQ |      |      |                |      |      |                                      |

Healthy ranges (min, max, and mean) describe known and expected values in a healthy subject. Parameters that are expected to change under hypoxic conditions are reported in the last column. We do not differentiate between adults and children. cHb, hemoglobin concentration; FiO<sub>2</sub>, fraction of inspired O<sub>2</sub>; P<sub>atm</sub>, atmospheric pressure; P<sub>ACO<sub>2</sub></sub>, alveolar partial pressure of carbon dioxide; PAO<sub>2</sub>, alveolar partial pressure of oxygen; PH<sub>2</sub>O: vapor pressure of water; RQ, respiratory quotient; SpO<sub>2</sub>, peripheral oxygen saturation; VS<sub>diff</sub>, diffusion defect; VS<sub>perf</sub>, perfusion defect. \*Same value range (min – max) assumed as at sea level.

concentration (cHb), alveolar partial pressure of carbon dioxide (P<sub>ACO<sub>2</sub></sub>), and the respiratory quotient (RQ). In addition, we divided VS into two components (Fig. 1): 1) incomplete capillary diffusion (diffusion defect between the alveolar and end-capillary compartments, VS<sub>diff</sub>) and 2) incomplete perfusion with intrapulmonary shunt (perfusion defect, VS<sub>perf</sub>).

We made the following assumptions for the model of a healthy subject: there is no oxygen loss between the alveoli and the end-capillaries (no incomplete capillary diffusion, VS<sub>diff</sub> = 0) and SpO<sub>2</sub> is equal to SaO<sub>2</sub> (24). These assumptions had the following consequences: the alveolar oxygen partial pressure (PAO<sub>2</sub>) is equal to the partial pressure of oxygen in the end-capillaries, the alveolar oxygen saturation is equal to the end-capillaries oxygen saturation, and the oxygen content in the alveoli is the same as the in the end-capillaries. For the parameters cHb and RQ, we extracted the healthy values at two altitudes (0 m and 4,600 m a.s.l.) from the literature (31, 32, 43) and linearly interpolated the parameters between these two altitudes. A linear interpolation was chosen because a sensitivity analysis revealed only small changes upon variation of these parameters (see APPENDIX). For high altitudes (i.e., 4,600 m a.s.l.), P<sub>ACO<sub>2</sub></sub> was derived from an interpolation of values reported by Rahn and Otis (35) and de Meer et al. (32), because the literature presented less coherent values; for sea level, direct values from Marcandante and Kliegman (30) and West (43) were used. With this information, the oxygen cascade enabled us to estimate the expected SpO<sub>2</sub> range at a specific altitude. Furthermore, we incorporated the technical tolerances that accounted for the accuracy of pulse oximeters (i.e. ± 2%) determined according to device standards (21) into the model, as shown in Karlen et al. (24). The pulse oximeter accuracy is an important component that is frequently neglected by health practitioners, but influences the pulse oximeter readings and therefore diagnostic results. We include this uncertainty in our model as we strive to describe better the physiology of lung function at different altitudes. Therefore, in the following, when we mention the “healthy ranges,” we refer to the physiological ranges obtained by modeling SpO<sub>2</sub> based on minimum and maximum literature values of the physiological parameters combined with the pulse oximeter inaccuracies.

#### *Altitude-Adaptive Abnormal SpO<sub>2</sub> Threshold*

Analogously, we derive an altitude-dependent threshold for abnormal SpO<sub>2</sub> by setting model parameters to hypoxemia

levels. Hypoxemia is defined as a reduced arterial partial pressure of oxygen (PaO<sub>2</sub>), which results in a decrease of SpO<sub>2</sub> and an increase of VS (43). At sea level, as reported in literature, we consider a patient to have hypoxemia if the PaO<sub>2</sub> level is below 80 mmHg (3, 26), and therefore SpO<sub>2</sub> decreases below 95%. Additionally, we assumed that VS<sub>perf</sub> increases to above 5% under hypoxemia (31). From these assumptions, we recursively derived a disease-related increase of VS<sub>diff</sub> of 19% at sea level. For higher altitudes, we were unable to retrieve any data from the literature that would describe changes (increase or decrease) in VS (VS<sub>diff</sub> or VS<sub>perf</sub>) or a numerical value for PaO<sub>2</sub> or PAO<sub>2</sub> under hypoxemia. Therefore, we assumed that the VS components remain constant across altitudes, and the values for cHb, P<sub>ACO<sub>2</sub></sub>, and RQ are similar in healthy and hypoxic conditions.

#### MATERIALS AND METHODS

To assess the performance and plausibility of our novel altitude-adaptive SpO<sub>2</sub> model and threshold, we retrospectively evaluated them against a prospectively collected data set, a previously published data set, and another statistical model with threshold.

#### *Study Design and Data Collection*

Our data collection was embedded within a randomized controlled trial by the Swiss-Peruvian Health Research Platform set in the Cajamarca region in the northern highlands of Peru located in the provinces of San Marcos and Cajabamba. Our study harnessed the operational and logistical setup of this trial, which assessed the efficacy of an Integrated Home-environmental Intervention Package (IHIP-2) to improve child respiratory, enteric, and early development outcomes (19).

The trial was approved by the Universidad Peruana Cayetano Heredia ethical review board and the Cajamarca Regional Health Authority. The trial was registered on the ISRCTN registry (ISRCTN26548981). A total of 317 children aged between 6 and 36 mo were enrolled, and informed written consent was obtained from the children’s guardians. A total of 9 field workers (FWs) were trained to visit the children on seven fixed geographical routes. Children were preassigned to these routes and visited in parallel by FWs to perform a mobile health assessment once a week over the course of 60 wk (6 wk pilot, followed by a 54-wk trial from February 2016 to May 2017, excluding 4 wk of public holidays). FWs had experience from earlier research projects in collecting basic vital signs and symptoms (17, 18), received 5 additional days of educational training for the collection of morbidity data, and underwent 1 month of practical training before the study started (pilot). FWs were equipped with a TAB 2 A7–10 tablet

(Lenovo Group Ltd.). The tablet had a custom mHealth app installed that was developed using the *lambdanative* framework (34). It recorded a photoplethysmogram (PPG) using a USB connected CE marked iSpO<sub>2</sub> Rx pulse oximeter (Masimo International) with a multisite Y-probe and derived SpO<sub>2</sub> and heart rate (HR). FWs placed the probe on the child's thumb, index finger, or sole of the foot for the measurement of PPG, HR, and SpO<sub>2</sub>. Simultaneously, respiratory rate was recorded using the RRate app module (22). In addition, the app acquired location and altitude using the embedded global positioning system (GPS) sensor. Furthermore, the app metadata regarding the visit and the recordings such as child identification, timestamps, and child agitation during the vital signs measurements were acquired. All electronically collected data were uploaded from the app into a digital research database (16). Health-seeking behavior and other relevant end points were reported in a paper-based, validated questionnaire (18), quality checked, and digitized at the end of the study.

### Postprocessing

The IHIP-2 vital signs data obtained from the pulse oximeter were postprocessed to guarantee high data quality. The PPG, SpO<sub>2</sub>, HR, and perfusion index (PI; indication of signal strength) time series from the main trial period were imported into Matlab (R2017b, MathWorks Inc., Natick, MA) where a signal quality index (SQI) for the PPG was calculated (23). We segmented the recordings into segments with SQI > 45. Segments with lower quality (SQI ≤ 45) and with no computed SpO<sub>2</sub> were excluded. Furthermore, entire recordings were excluded if a single segment duration was shorter than 12 s or the combined length of remaining segments was shorter than 15 s, the range (5th–95th centile) of SpO<sub>2</sub> exceeded 5%, and the HR range surpassed 20 beats/min in combination with a low perfusion (mean PI ≤ 0.8). We also excluded SpO<sub>2</sub> values below 60% as they are rare and typically associated with severe clinical cyanosis (46), which was clearly absent in the IHIP-2 cohort. These values also fall in a range where the performance of the pulse oximeters used were not specified by the manufacturer (70% to 100%). Additionally, as each child was always scheduled to be measured weekly at the same altitude (i.e., at home), we verified the consistency of the altitude provided by the GPS. We excluded recordings that contained no altitude information, and altitude outliers that were more than three scaled median absolute deviations away from the median altitude of each child. Altitude outliers could have occurred because at-home measurements were not always possible and because GPS altitude estimates were dependent on weather, the number of available satellites, and other factors. Finally, we excluded measurements that were recorded following a healthcare center visit or the presence of cardiorespiratory or diarrheal disease symptoms in the week preceding the recording. For each remaining high quality recording, we reported the median SpO<sub>2</sub> over the combined segments of a measurement and the median altitude per child, which was then used for the analysis.

### Evaluation

**Model.** To compare our model with the available data sets, we visualized the altitude dependence of SpO<sub>2</sub>. We applied a locally weighted scatterplot smoothing (lowess) function (5) to all SpO<sub>2</sub>-altitude data pairs collected during the IHIP-2 trial. We limited the comparison to the range of available data (2,000–4,000 m a.s.l.) to avoid extrapolation errors. Instead of the LSM method used by Rojas-Camayo et al. (36), we reported the centiles of their data with a lowess smoother to ensure equivalent processing of both data sets. Furthermore, we computed the deviations from interpolated medians of both empirical data sets to the model median for each altitude expressed as percent of the respective model value and reported the mean, minimum, and maximum deviations. Additionally, we calculated the absolute range

of SpO<sub>2</sub> values at each altitude for both the model and the empirical data sets and reported mean, minimum, and maximum range.

**Threshold.** To visualize the differences between the hypoxemia/abnormal SpO<sub>2</sub> thresholds and oxygen administration guidelines that have been proposed, we graphically compared the altitude-adaptive abnormal SpO<sub>2</sub> threshold, the statistical hypoxemia threshold, and the WHO guideline for oxygen administration (90%) with the 2.5th centile (lowess smoothed) data of children 1 to 5 yr old reported by Rojas-Camayo et al. (36). We further computed the number of measurements in the healthy IHIP-2 data that would have been wrongly classified as abnormal (false positives) when using either the altitude-adaptive abnormal SpO<sub>2</sub> threshold or the statistical hypoxemia threshold. The false positives are children that are healthy, but likely would receive additional medical attention due to the low SpO<sub>2</sub> reading.

## RESULTS

We obtained an altitude-adaptive computer model to describe the expected SpO<sub>2</sub> range in healthy children at higher altitudes and, based on this model, proposed a threshold for an abnormal range that could indicate hypoxemia. The parameters used in the mathematical description of the model to define healthy and abnormal ranges are available in Table 1. Out of the 12,634 SpO<sub>2</sub> measurements obtained from 310 children over the course of a year, we retained 5,981 measurements from 297 children that were considered complete (contained both GPS and PPG data), featured good quality PPG data, reasonable SpO<sub>2</sub> (>60%), and were recorded when no respiratory disease symptoms or other health issues were reported (410 recordings). At the study start, the mean age of the children was 20.5 mo (SD 6.2 mo, range: 6–36 mo). Each child contributed to a mean of 20.1 (SD 9) repeated measurements. Twenty-one children lived above 3,000 m a.s.l. and 8 above 3,500 m a.s.l. (Table 2). Therefore, a total of 392 (6.6%) measurements above 3,000 m a.s.l. was available.

### Model

Our altitude-adaptive model provided an SpO<sub>2</sub> of 97.4% at sea level with a healthy range between 93.5% and 100% SpO<sub>2</sub> [Fig. 2 and Table 3, high-resolution data including model available at (11)]. The SpO<sub>2</sub> of the model decreased with increasing altitude to 89.6% at 4,000 m a.s.l., with a healthy SpO<sub>2</sub> range from 82.3% to 94.1%. The 2.5th and 97.5th centiles reported by Rojas-Camayo et al. largely followed the same trend as those acquired in the IHIP-2 trial, but had a smaller absolute range (Fig. 2). Up to 3,800 m a.s.l., the 2.5th centiles of both empirical data sets were entirely within the lower boundary of the altitude-adaptive SpO<sub>2</sub> model's proposed healthy range, whereas at higher altitudes above 3,800 m a.s.l., the 2.5th centile of the IHIP-2 data slightly fell below this lower boundary. The upper boundary of the altitude-adaptive SpO<sub>2</sub> model's healthy range followed the IHIP-2 data 97.5th centile closely, while it was slightly exceeded by the 97.5th centile data from Rojas-Camayo et al. between 1,500 and 3,100 m a.s.l. by up to 0.5%. In particular, the model showed absolute ranges very similar to both empirical lowess filtered data sets (model: mean absolute SpO<sub>2</sub> range: 8.66%, min: 6.42%, max: 11.78%; IHIP-2: mean absolute SpO<sub>2</sub> range: 8.75%, min: 6.75%, max: 11.22%; Rojas-Camayo: mean absolute SpO<sub>2</sub> range: 5.53%, min: 3.43%, max: 8.92%). Furthermore, the model differed very little from the interpolated median of the empirical data sets (IHIP-2, deviation

Table 2. IHIP-2 pulse oximeter data

| Altitude, m a.s.l. | No. Children | Age at Study Start, mo |     | No. of Measurements | No. of Measurements per Child |      |     | SpO <sub>2</sub> , % |        |       |
|--------------------|--------------|------------------------|-----|---------------------|-------------------------------|------|-----|----------------------|--------|-------|
|                    |              | Mean                   | SD  |                     | Min                           | Mean | Max | Min                  | Median | Max   |
| 2,000              | 78           | 21.0                   | 6.0 | 1,668               | 1                             | 21.4 | 39  | 88.9                 | 97.2   | 100.0 |
| 2,100              | 37           | 20.4                   | 6.1 | 803                 | 1                             | 21.7 | 43  | 87.4                 | 97.2   | 100.0 |
| 2,200              | 6            | 15.7                   | 5.0 | 109                 | 7                             | 18.2 | 24  | 88.6                 | 96.6   | 99.7  |
| 2,300              | 15           | 19.5                   | 6.7 | 389                 | 5                             | 25.9 | 34  | 89.2                 | 96.7   | 100.0 |
| 2,400              | 3            | 24.0                   | 2.0 | 77                  | 19                            | 25.7 | 31  | 91.9                 | 96.2   | 100.0 |
| 2,500              | 13           | 20.5                   | 5.7 | 264                 | 4                             | 20.3 | 33  | 87.1                 | 96.0   | 100.0 |
| 2,600              | 22           | 21.6                   | 5.6 | 472                 | 2                             | 21.5 | 39  | 81.1                 | 96.0   | 100.0 |
| 2,700              | 39           | 21.5                   | 6.8 | 753                 | 4                             | 19.3 | 32  | 85.2                 | 95.6   | 100.0 |
| 2,800              | 20           | 21.8                   | 5.7 | 316                 | 1                             | 15.8 | 34  | 83.9                 | 95.2   | 99.5  |
| 2,900              | 18           | 17.7                   | 6.0 | 276                 | 1                             | 15.3 | 27  | 85.6                 | 94.7   | 98.6  |
| 3,000              | 25           | 20.2                   | 7.2 | 462                 | 5                             | 18.5 | 37  | 81.5                 | 94.5   | 100.0 |
| 3,100              | 8            | 20.0                   | 6.5 | 111                 | 1                             | 13.9 | 24  | 80.7                 | 94.4   | 100.0 |
| 3,200              | 3            | 19.3                   | 6.0 | 76                  | 12                            | 25.3 | 38  | 85.7                 | 93.4   | 98.2  |
| 3,300              | 1            | 20.0                   | 0.0 | 19                  | 19                            | 19.0 | 19  | 89.9                 | 92.4   | 95.7  |
| 3,400              | 1            | 17.0                   | 0.0 | 15                  | 15                            | 15.0 | 15  | 86.0                 | 92.9   | 95.4  |
| 3,500              | 0            |                        |     | 0                   |                               |      |     |                      |        |       |
| 3,600              | 5            | 19.4                   | 4.7 | 107                 | 9                             | 21.4 | 30  | 84.3                 | 92.7   | 98.7  |
| 3,700              | 1            | 28.0                   | 0.0 | 24                  | 24                            | 24.0 | 24  | 86.4                 | 92.5   | 95.6  |
| 3,800              | 1            | 23.0                   | 0.0 | 22                  | 22                            | 22.0 | 22  | 80.8                 | 87.8   | 93.9  |
| 3,900              | 1            | 14.0                   | 0.0 | 18                  | 18                            | 18.0 | 18  | 81.6                 | 88.4   | 90.6  |
| Total              | 297          | 20.5                   | 6.2 | 5,981               | -                             | 20.1 | -   | -                    | -      | -     |

Distribution of children, number of measurements, and peripheral oxygen saturation (SpO<sub>2</sub>) per altitude. Age range of the children at study start: 6–36 mo (mean: 20.5 mo, SD: 6.2 mo), 21 children above 3,000 m a.s.l. (392 measurements, 6.6% of total number of measurements), 8 above 3,500 m a.s.l. (171 measurements, 2.9% of total number of measurements), mean number of measurement per child: 20.1 (SD 9).

of model in percent: mean deviation: 1.5%, min: 0.01%, max: 2.29%; Rojas-Camayo: mean deviation: 1.51%, min: 0.02%, max: 1.95%.

**Threshold**

The altitude-adaptive abnormal SpO<sub>2</sub> threshold followed a similar pattern as the 2.5th centile of Rojas-Camayo’s empir-

ical data with 88.8% versus 94% at 2,000 m a.s.l. and 80.1% versus 83.8% at 4,000 m a.s.l. (Fig. 3, see also Table 3). The 2.5th centile threshold explored by Subhi et al. had an SpO<sub>2</sub> of 92.8% at 2,000 m a.s.l. and then rapidly diverged toward much lower SpO<sub>2</sub> values for higher altitudes (75.4% at 4,000 m a.s.l.). When comparing the two thresholds and their performance for our empirical data set, the altitude-adaptive thresh-

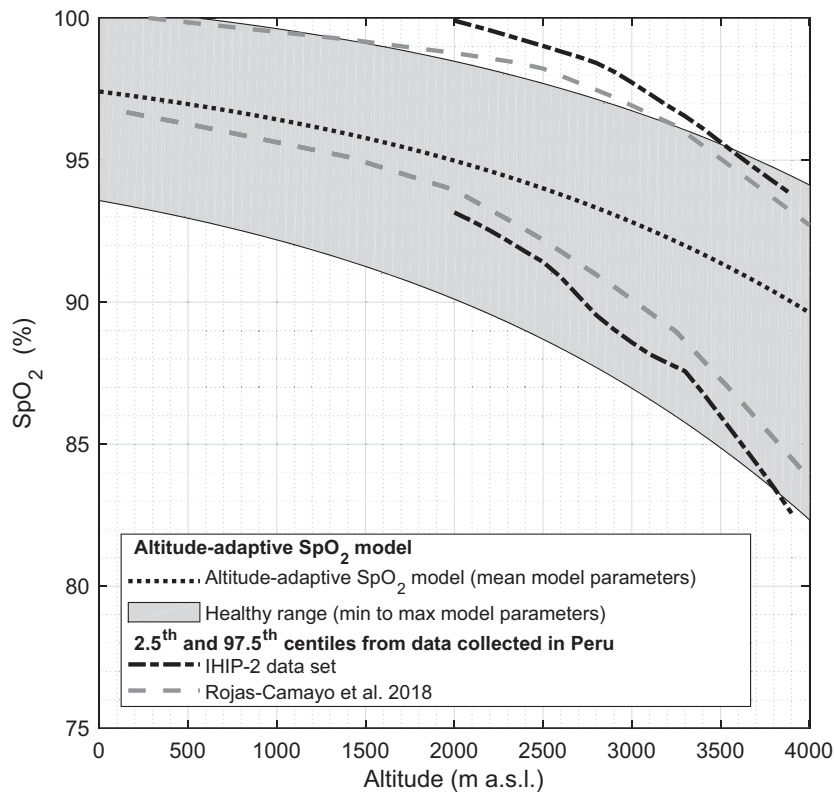


Fig. 2. Proposed altitude-adaptive peripheral oxygen saturation (SpO<sub>2</sub>) model provides a healthy SpO<sub>2</sub> range (light gray area). Black dotted line indicates the median SpO<sub>2</sub> estimated by the model. Parameters for the min, max, and mean model parameters are given in Table 1. The 2.5th–97.5th centiles of the SpO<sub>2</sub> data are from Rojas-Camayo et al. (36; gray dashed lines) and the Integrated Home-environmental Intervention Package (IHIP-2) data set (black dashed-dotted lines) that were both recorded in the Peruvian Andes mostly fall into our proposed healthy range. Reported number of measurements per children for the IHIP-2 data can be found in Table 2.

Table 3. Values of the healthy ranges of the altitude-adaptive SpO<sub>2</sub> model, including its median and the abnormal SpO<sub>2</sub> threshold, per altitude

| Altitude, m a.s.l. | Upper Healthy Range, %SpO <sub>2</sub> | Lower Healthy Range, %SpO <sub>2</sub> | Model Mean, %SpO <sub>2</sub> | Threshold, %SpO <sub>2</sub> |
|--------------------|--|--|-------------------------------|------------------------------|
| 0                  | 100.0                                  | 93.6                                   | 97.4                          | 92.9                         |
| 500                | 100.0                                  | 93.0                                   | 97.0                          | 92.2                         |
| 1,000              | 99.6                                   | 92.2                                   | 96.4                          | 91.2                         |
| 1,500              | 99.1                                   | 91.3                                   | 95.8                          | 90.1                         |
| 2,000              | 98.5                                   | 90.1                                   | 95.0                          | 88.8                         |
| 2,500              | 97.7                                   | 88.7                                   | 94.0                          | 87.1                         |
| 3,000              | 96.7                                   | 87.0                                   | 92.8                          | 85.2                         |
| 3,500              | 95.6                                   | 84.9                                   | 91.4                          | 82.9                         |
| 4,000              | 94.1                                   | 82.3                                   | 89.6                          | 80.1                         |

SpO<sub>2</sub>, peripheral oxygen saturation. More granular altitude steps available in (11).

old estimated abnormal SpO<sub>2</sub> in only 17 of 5,981 (0.3%) healthy recordings, whereas the 2.5th centile threshold explored by Subhi et al. returned 95 (1.6%) false positives.

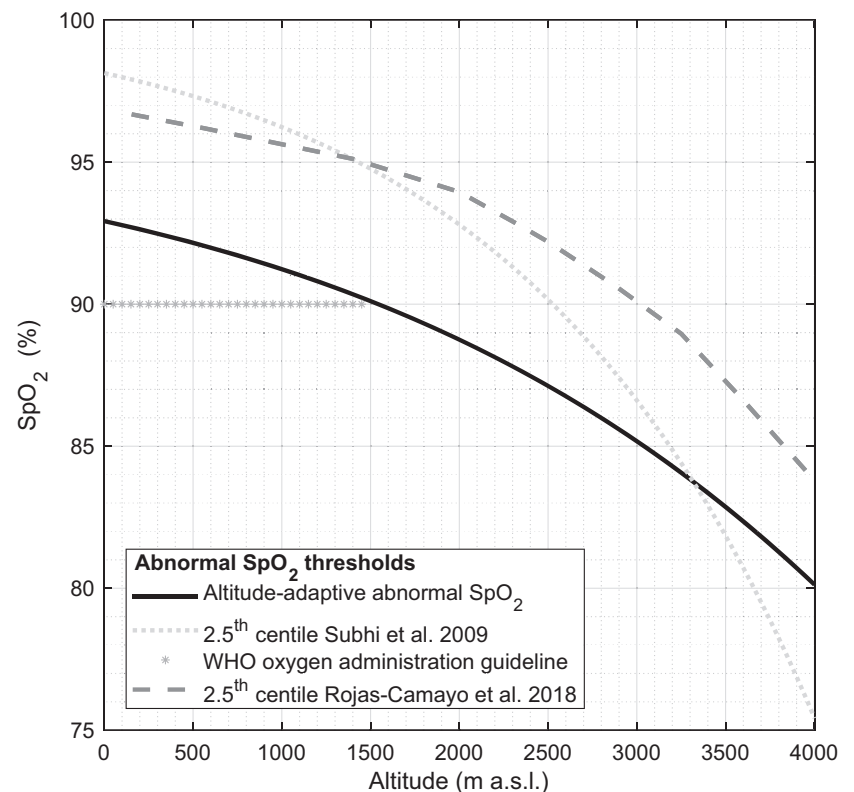
## DISCUSSION

We proposed an altitude-adaptive model that estimates a healthy SpO<sub>2</sub> range for children living permanently at altitude and have shown that this proposed healthy SpO<sub>2</sub> range matches empirical data recorded from a pediatric population living in the Andes. From this model, we derived an altitude-adaptive threshold for abnormal SpO<sub>2</sub> values. The diagnosis of pneumonia and other respiratory diseases is challenging at altitude, as the most common diagnostic criteria, such as the respiratory rate and oxygen saturation, are dependent on altitude. Our work contributes toward making the management of childhood pneumonia, one of the major causes of child mortality in low resource settings, more objective by attempting better to de-

scribe healthy changes of respiratory physiology found in adapted residents. Equipping health workers with mobile pulse oximeters has become an affordable solution, is being evaluated at a large scale (29), and has potential for improving pneumonia treatment at a reasonable cost (12). However, the measurement and interpretation of SpO<sub>2</sub> can be complicated. Computerized assistance and interpretation of the measurements could ensure reliability of these measurements and provide a meaningful decision support tool to health workers at the central and peripheral level. The proposed adaptive, physiology-based model could provide a basis for the necessary computations because it provides a reference for healthy values at higher altitudes.

Our model is unique as the adjustment of the parameters can be tuned individually, based either on measurements or on known parameter ranges, and it is based on physiology. It was developed considering, where available, literature-based phys-

Fig. 3. Comparison of proposed abnormal peripheral oxygen saturation (SpO<sub>2</sub>) thresholds that would lead to oxygen administration in patients and existing guidelines. The altitude-adaptive abnormal SpO<sub>2</sub> threshold (continuous black line) is based on the physiological model derived in this work where a virtual shunt was applied. The threshold from Subhi et al. (40) is the 2.5th centile derived from observations in healthy children collected in a literature review (dotted gray line), and the 2.5th centile from Rojas-Camayo et al. (36) is derived from a prospectively collected healthy pediatric sample in the Peruvian Andes (dashed gray line). The World Health Organization (WHO) 90% oxygen administration guideline (44) is a result of a working group consensus (starred gray line) that is in use at lower altitudes.



iological parameter values of Peruvian Andes residents that are adapted to this environment. These parameters could be adjusted without altering the underlying model for other populations with known differences in genetic or physiological adaptation mechanisms (e.g., Himalayan residents) (1).

In contrast to our parameterized model, Subhi and colleagues (40) fitted empirical data collected from across the world into a statistical model describing the SpO<sub>2</sub> distribution using centiles. The statistical model was built using aggregated data collected from mixed populations using pulse oximeters with partially unknown specifications. The statistical model therefore cannot be adjusted to factors such as population-specific variations or varying technical specifications (e.g., differing accuracy of pulse oximeter brands or types). In relation to the two empirical data sets mentioned in this publication, and in comparison to our proposed abnormal SpO<sub>2</sub> threshold, the statistical threshold provided a very sensitive cut-off at lower altitudes (up to 3,300 m a.s.l.). However, it underestimates potentially abnormal SpO<sub>2</sub> values at higher altitudes. Most likely, this underestimation of the abnormal SpO<sub>2</sub> values at higher altitudes is due to fewer data samples being available for the statistical modeling. Our physiological model was not affected by data sparsity, which is a distinctive feature and clear advantage at higher altitudes. Both model thresholds and the studied data sets supported the current WHO constant threshold of 90% SpO<sub>2</sub> for oxygen administration at altitudes below 1,500 m a.s.l.

The altitude-adaptive model described the SpO<sub>2</sub> ranges observed from the empirical data sets with highly similar mean absolute ranges. However, the two empirical data sets presented in this work originate solely from the Peruvian Andes and a single type of pulse oximeter. To further validate the model, it will be crucial to apply data from other regions and ethnicities and establish if a customized model is required when used in different parts of the world. Such data collection should be accompanied by a gold standard, such as blood gas measurements with information on cHb, SaO<sub>2</sub>, PaO<sub>2</sub>, and PaCO<sub>2</sub> to pinpoint the exact sources of potentially observed differences.

At higher altitudes above 3,800 m a.s.l., we notice higher deviations in the model compared with what is seen in the empirical data due to a slower decline of SpO<sub>2</sub> in the model. We suspect that this is directly linked to the assumptions we made during the modeling of healthy ranges. We assumed that cHb and RQ change linearly with altitude. However, the adaptation process is likely more pronounced at higher altitudes (6) and might contribute to nonlinear parameter changes.

Our assumptions to define the abnormal physiological parameters could limit the validity of the abnormal threshold. We only based our assumptions on literature values that referred to sea level patients. Due to the underlying changes in physiology caused by adaptation, disease manifestation, and progression, symptoms could be different at high altitudes compared with at sea level. Furthermore, it is unclear if comorbidities that have not been captured in the present modeling, such as malnutrition, iron deficiency, or diarrheal diseases that are known to negatively influence outcomes of patients with pneumonia (4, 37, 39), would also influence the model parameters. Additional empirical data of sick children are needed to establish models that describe the dependence of these parameters to altitude. For example, anemic children display altered ranges for blood gas

parameters and their actual health status is not entirely captured through our cardiorespiratory model based on SpO<sub>2</sub> measurements. SpO<sub>2</sub> and derived hypoxemia estimations reflect only the proportion of O<sub>2</sub> that is bound to Hb and not the total O<sub>2</sub> carrying capacity and concentration. Consequently, pulse oximeter assessments are blind to the effective O<sub>2</sub> available in the tissues. Also, cardiac output, an alternative path to modulate O<sub>2</sub> delivery (14), is not easily obtainable with pulse oximetry alone. Thus, clinicians need to take the overall clinical situation of the child into consideration and evaluate treatment options accordingly when interpreting hypoxemia thresholds (10).

To assess the performance of the model, we limited the comparison to altitudes from 2,000 to 4,000 m a.s.l. where corresponding empirical data were available. The data contained weekly measurements for each child repeated over a full year (mean: 20.1, SD: 9), therefore representing the expected measurement and physiological variability within a healthy subject. Among the children recruited from the Cajamarca region during the IHIP-2 trial, only 21 lived above 3,000 m a.s.l., which increases the variability in the data. Nevertheless, we observed very similar SpO<sub>2</sub> ranges from Rojas-Camayo et al. (36). Despite the high numbers of repeated measurements and rigid measurement protocols, both data sets showed a high variability in the measured SpO<sub>2</sub>. For example, in the IHIP-2 data set, at 2,000 m a.s.l. a healthy range corresponded to 11% (Table 2). Our model represented this large range of possible healthy values accurately. Nevertheless, the inter- and intra-individual variability could originate from a number of sources not incorporated in the model. Circadian variation in pediatric SpO<sub>2</sub> has been reported (42), and we did not account for such daytime differences. Furthermore, there are known sex differences in adults (1), which could also apply to the pediatric population. Although we used the most recent pulse oximeter technology and performed continuous measurements for at least a minute with a rigorous approach to PPG postprocessing for high quality, not all the sources for measurement errors in pulse oximetry, such as poor perfusion, inaccurate probe positioning, or ambient light interference (13), could be fully excluded in this data set.

Additionally, it is important to note that neonates were not considered in the modeling process. Neonatal blood is known to benefit from the high affinity of fetal hemoglobin and would have changed the oxygen dissociation curve considerably (33). Since hyperoxia in neonates leads to oxidative stress with potentially severe health complications (15), the definition of an abnormal threshold and consequently the guideline for oxygen administration would require a more detailed, separate discussion for this population.

We established an altitude-adaptive abnormal SpO<sub>2</sub> threshold based on physiologically plausible values. Our results show that using such a threshold is most relevant at altitudes above 2,000 m a.s.l. The 90% SpO<sub>2</sub> threshold recommended by the WHO for oxygen administration in patients living at sea level clearly does not apply to these altitudes. Compared with the previously published statistical altitude-dependent threshold by Subhi et al. (40), our threshold leads to fewer detections of false positives (healthy children falsely categorized as hypoxic). Conversely, while Subhi et al. also promoted the use of an altitude-dependent threshold at higher altitudes (2,500 m a.s.l.), their threshold is very conservative at altitudes below

2,950 m a.s.l. but more lenient at higher altitudes, where it decreases very steeply, which might exclude a number of patients in need of supplemental oxygen.

### Outlook

Thus far, experts have not agreed on a definition for abnormal SpO<sub>2</sub> thresholds at altitudes higher than sea level. To date, no reliable SpO<sub>2</sub> data from children suffering from hypoxemia and ALRI at altitude are available. The advancement of research for developing better tools to diagnose pneumonia and ALRI at altitude would greatly benefit from access to publicly available, comprehensive data sets obtained from sick children.

With pulse oximeters increasingly being used as monitors for ALRI diagnosis and treatment, additional research is urgently needed to provide a reliable description of the SpO<sub>2</sub> distribution at altitude and to develop guidelines of oxygen administration for hypoxemic children living in these settings.

Furthermore, knowledge of abnormal SpO<sub>2</sub> values at high altitudes could help in the development of new decision support tools for health workers operating in low resource settings with the goal to improve clinical management of hypoxemia in children with ALRI in the future.

### Conclusions

Improvement of SpO<sub>2</sub>-altitude models presents a first step toward an integration of pulse oximetry in low resource settings and could further the development of valid altitude-dependent thresholds for treatment of childhood pneumonia and other ALRI. We developed an altitude-adaptive physiology-backed SpO<sub>2</sub> model using an existing physiological model using the concept of VS adjusted for published ranges of values for P<sub>ACO<sub>2</sub></sub>, cHb, and RQ. With this model, healthy ranges and an altitude-dependent abnormal SpO<sub>2</sub> threshold are suggested that are based on physiological variations of vital parameters. With the increased availability of sensors and digitalized systems in low resource settings, parametrized models could provide additional valuable support to primary health workers to understand the patient's condition at the point of care and to

choose treatment options based on objectively obtained physiological measurements.

### APPENDIX

Parameters required for the calculation of the oxygen cascade with specification of dependency on other parameters and the expected change with increasing altitude are shown in Table A1.

#### Equations

For the entire computer model of the oxygen cascade, please consult (24, 25). See Table A1 for the variable names.

*Alveolar gas equation.*

$$P_{A_{O_2}} = F_{i_{O_2}} * (P_{atm} - P_{H_2O}) - \frac{P_{A_{CO_2}}}{RQ} + P_{A_{CO_2}} * F_{i_{O_2}} * \frac{1 - RQ}{RQ}$$

where P<sub>atm</sub> is the ambient gas pressure and P<sub>H<sub>2</sub>O</sub> is the vapor pressure of Water.

*Severinghaus equation (38).*

$$S_{A_{O_2}} = \frac{1}{\frac{23,400}{P_{A_{O_2}}^3 + 150 * P_{A_{O_2}}} + 1} * 100$$

where S<sub>A<sub>O<sub>2</sub></sub> is the oxygen saturation of the alveolar blood.</sub>

*O<sub>2</sub> content equation.*

$$C_{x_{O_2}} = BO_2 * \frac{cHb * S_{x_{O_2}}}{100} + 0.003 * P_{x_{O_2}}$$

where BO<sub>2</sub> is Oxygen-binding capacity of hemoglobin in blood and x denotes a placeholder for the respective compartment.

*Severinghaus-Ellis equation (9).*

$$P_{A_{O_2}} = (B + A)^{1/3} - (B - A)^{1/3}$$

where

$$A = \frac{11,700}{\frac{1}{S_{A_{O_2}} - 1}} \quad \text{and} \quad B = \sqrt{50^3 + A^2}$$

Table A1. Parameters required for the calculation of the oxygen cascade with specification of dependency on other parameters and the expected change with increasing altitude

| Abbreviation  | Unit                      | Name   | Healthy Adult Value at 0 m a.s.l. | Dependency  | Expected Change with Increasing Altitude |
|---|---------------------------|--|-----------------------------------|---|--|
| P <sub>A<sub>O<sub>2</sub></sub></sub>                    | mmHg                      | Partial pressure of alveolar O <sub>2</sub>                                  |                                   | F <sub>i<sub>O<sub>2</sub></sub></sub> , P <sub>atm</sub> , P <sub>H<sub>2</sub>O</sub> , P <sub>ACO<sub>2</sub></sub> and RQ | Decrease                                 |
| S <sub>c'<sub>O<sub>2</sub></sub></sub>                   | %                         | Oxygen saturation of end-capillary blood                                     |                                   | P <sub>A<sub>O<sub>2</sub></sub></sub>  | Decrease                                 |
| C <sub>c'<sub>O<sub>2</sub></sub></sub>                   | ml/100 ml                 | Oxygen content of end-capillary blood  |                                   | BO <sub>2</sub> , cHb, S <sub>A<sub>O<sub>2</sub></sub></sub> , P <sub>A<sub>O<sub>2</sub></sub></sub>                        | Increase                                 |
| Ca <sub>O<sub>2</sub></sub>                               | ml/100 ml                 | Oxygen content of arterial blood   |                                   | BO <sub>2</sub> , cHb, S <sub>A<sub>O<sub>2</sub></sub></sub> , P <sub>A<sub>O<sub>2</sub></sub></sub>                        | Increase                                 |
| Pa <sub>O<sub>2</sub></sub>                               | mmHg                      | Partial pressure of arterial O <sub>2</sub>                                  |                                   | S <sub>A<sub>O<sub>2</sub></sub></sub>  | Decrease                                 |
| S <sub>A<sub>O<sub>2</sub></sub></sub>                    | %                         | Oxygen saturation of arterial blood  |                                   |   | Decrease                                 |
| P <sub>atm</sub>  | kPa                       | Ambient gas pressure   | 101.325                           |   | Decrease                                 |
| F <sub>i<sub>O<sub>2</sub></sub></sub>                    | %                         | Fraction of inspired O <sub>2</sub>  | 21                                |   | No change                                |
| P <sub>ACO<sub>2</sub></sub>                              | mmHg                      | Partial pressure of alveolar CO <sub>2</sub>                                 | 40                                |   | Decrease                                 |
| VS <sub>perf</sub>  | %                         | Perfusion component of virtual shunt   | 2                                 |   | No change                                |
| VS <sub>diff</sub>  | %                         | Diffusion component of virtual shunt   | 0                                 |   | No change                                |
| RQ  | unitless                  | Respiratory exchange ratio (O <sub>2</sub> inspired/CO <sub>2</sub> expired) | 0.8                               |   | Increase                                 |
| cHb   | g/100 ml                  | Hemoglobin concentration in blood  | 12                                |   | Increase                                 |
| P <sub>H<sub>2</sub>O</sub>                               | mmHg                      | Vapor pressure of water  | 47                                |   | No change                                |
| BO <sub>2</sub>   | ml O <sub>2</sub> /(g Hb) | Oxygen-binding capacity of hemoglobin in blood                               | 1.34                              |   | No change                                |
| Ca <sub>O<sub>2</sub></sub> - Cv <sub>O<sub>2</sub></sub> | ml/100 ml                 | Arteriovenous oxygen difference  | 5                                 |   | No change                                |

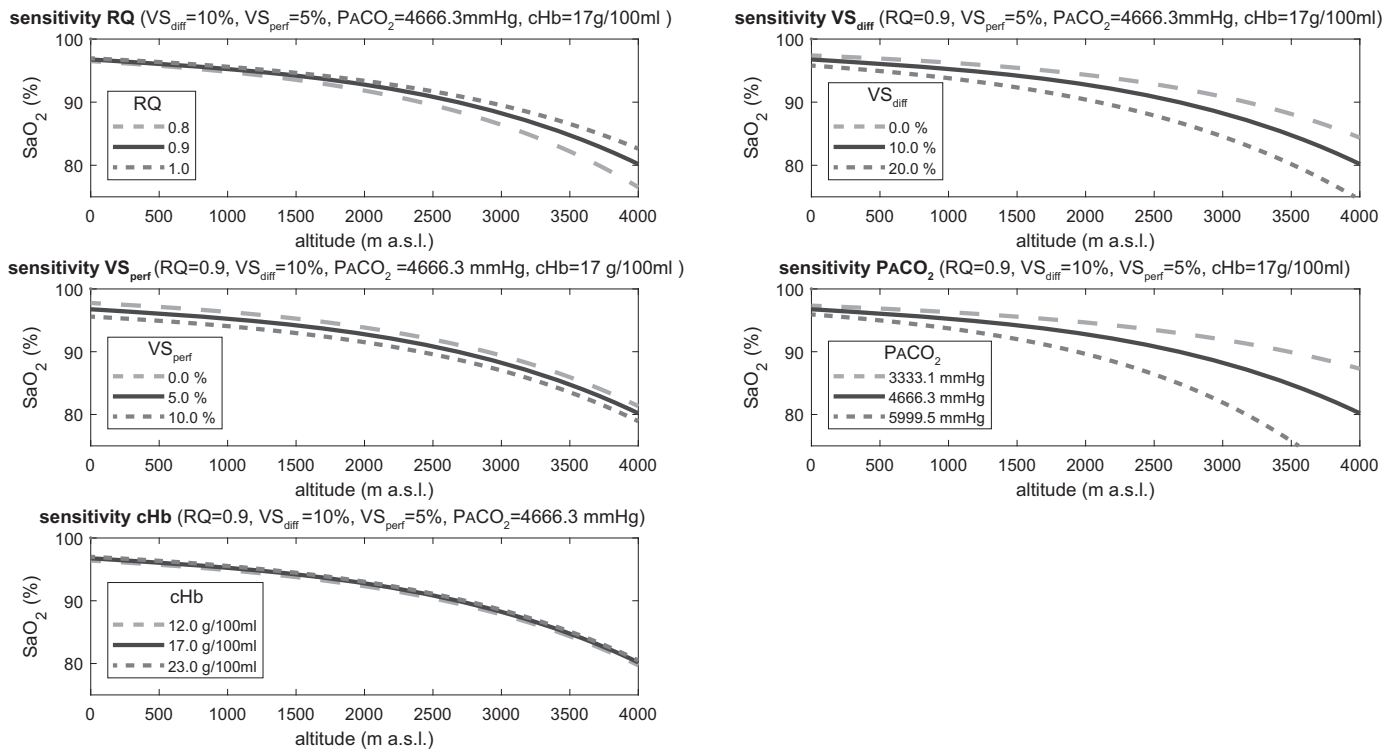


Fig. A1. Sensitivity analysis of the 5 main model parameters respiratory quotient (RQ) (*top left*), virtual shunt from diffusion defect ( $VS_{diff}$ ) (*top right*), virtual shunt from perfusion defect ( $VS_{perf}$ ) (*middle left*), alveolar partial pressure of carbon dioxide ( $PACO_2$ ) (*bottom right*), and hemoglobin concentration (cHb) (*bottom left*).  $PAO_2$ , alveolar partial pressure of oxygen;  $SaO_2$ , oxygen saturation in arterial blood.

Virtual shunt from perfusion defect ( $VS_{perf}$ ).

$$VS_{perf} = \frac{Cc'O_2 - CaO_2}{Cc'O_2 - CaO_2 + (CaO_2 - CvO_2)}$$

where  $Cc'O_2$  is oxygen content of end-capillary blood;  $CaO_2$  is oxygen content of arterial blood; and  $CvO_2$  is oxygen content of venous blood.

Virtual shunt from diffusion defect ( $VS_{diff}$ ).

$$Pc'O_2 = PAO_2 * (1 - VS_{diff})$$

where  $Pc'O_2$  is the O<sub>2</sub> partial pressure at the end-capillaries.

#### Sensitivity analysis

To display the influence of parameters on the output of the oxygen cascade, a sensitivity analysis was performed (Fig. A1). The parameter variation was chosen to reproduce the minimum and maximum value used in the altitude-adaptive SpO<sub>2</sub> model (Table 1). A change in  $PACO_2$  had the highest effect, followed by  $VS_{diff}$ ,  $VS_{perf}$ , and RQ. A change in cHb is negligible for the calculation of SpO<sub>2</sub>; however, please note that it has a significant influence on availability of O<sub>2</sub> in the tissues.

#### ACKNOWLEDGMENTS

We are grateful to all staff and students from the Swiss-Peruvian Health Research Platform and the San Marcos research station, especially Angelica Fernandez and Maria Luisa Huyalinos, Hector Verastegui, and Nestor Nuño for assistance and support throughout the study. The San Marcos Red Salud-IV health personnel supported the SpO<sub>2</sub> measurement in the peripheral health posts. Matthias Hüser programmed the assessment app and maintained the software throughout the study. We thank all the families that participated in the randomized trial. We thank Dr. Jose Rojas-Camayo for sharing the centiles of his valuable data set, Ms. Janine Burren for

valuable input on statistics and data representation, and Dr. Urs Frey and Joanne Lim for helpful comments on this manuscript. We appreciate the various contributions of the colleagues from the Swiss Pediatric Surveillance Unit (SPSU) network. Furthermore, Masimo International kindly facilitated the access to their pulse oximeter sensors in Peru.

#### GRANTS

The presented research was supported through ETH Global seed funding, the Swiss National Science Foundation (150640), and the UBS Optimus Foundation.

#### DISCLOSURES

No conflicts of interest, financial or otherwise, are declared by the authors.

#### AUTHOR CONTRIBUTIONS

S.M.H., D.M., and W.K. conceived and designed research; L.T., M.M., S.M.H., and W.K. interpreted results of experiments; L.T., M.M., J.Z., D.M., and W.K. drafted manuscript; L.T., J.Z., S.M.H., D.M., and W.K. edited and revised manuscript; L.T., M.M., J.Z., S.M.H., D.M., and W.K. approved final version of manuscript; M.M., J.Z., S.M.H., D.M., and W.K. performed experiments; M.M. and J.Z. analyzed data; L.T., M.M. and W.K. prepared figures.

#### ENDNOTE

At the request of the authors, readers are herein alerted to the fact that additional materials related to this manuscript may be found at the institutional Web site of the authors, which at the time of publication they indicate is at <https://doi.org/10.3929/ethz-b-000344084>. These materials are not a part of this manuscript and have not undergone peer review by the American Physiological Society (APS). APS and the journal editors take no responsibility for these materials, for the Web site address, or for any links to or from it.

## REFERENCES

1. Beall CM. Two routes to functional adaptation: Tibetan and Andean high-altitude natives. *Proc Natl Acad Sci USA* 104, Suppl 1: 8655–8660, 2007. doi:10.1073/pnas.0701985104.
2. Benatar SR, Hewlett AM, Nunn JF. The use of iso-shunt lines for control of oxygen therapy. *Br J Anaesth* 45: 711–718, 1973. doi:10.1093/bja/45.7.711.
3. Bradley JS, Byington CL, Shah SS, Alverson B, Carter ER, Harrison C, Kaplan SL, Mace SE, McCracken GH, Moore MR, St Peter SD, Stockwell JA, Swanson JT. The management of community-acquired pneumonia in infants and children older than 3 months of age: Clinical practice guidelines by the pediatric infectious diseases society and the infectious diseases society of America. *Clin Infect Dis* 53: e25–e76, 2011. doi:10.1093/cid/cir531.
4. Chisti MJ, Graham SM, Duke T, Ahmed T, Faruque ASG, Ashraf H, Bardhan PK, Shahid ASMSB, Shahunja KM, Salam MA. Post-discharge mortality in children with severe malnutrition and pneumonia in Bangladesh. *PLoS One* 9: e107663, 2014. doi:10.1371/journal.pone.0107663.
5. Cleveland WS, Devlin SJ. Locally weighted regression: an approach to regression analysis by local fitting. *J Am Stat Assoc* 83: 596–610, 1988. doi:10.1080/01621459.1988.10478639.
6. Cohen JH, Haas JD. Hemoglobin correction factors for estimating the prevalence of iron deficiency anemia in pregnant women residing at high altitudes in Bolivia. *Rev Panam Salud Publica* 6: 392–399, 1999. doi:10.1590/S1020-49891999001100004.
7. Duke T, Subhi R, Peel D, Frey B. Pulse oximetry: technology to reduce child mortality in developing countries. *Ann Trop Paediatr* 29: 165–175, 2009. doi:10.1179/027249309X12467994190011.
8. Duke T, Wandt F, Jonathan M, Matai S, Kaupa M, Saavu M, Subhi R, Peel D. Improved oxygen systems for childhood pneumonia: a multi-hospital effectiveness study in Papua New Guinea. *Lancet* 372: 1328–1333, 2008. doi:10.1016/S0140-6736(08)61164-2.
9. Ellis RK. Determination of PO<sub>2</sub> from saturation. *J Appl Physiol* (1985) 67: 902, 1989. doi:10.1152/jappl.1989.67.2.902.
10. Enoch AJ, English M, Shepperd S. Does pulse oximeter use impact health outcomes? A systematic review. *Arch Dis Child* 101: 694–700, 2016. doi:10.1136/archdischild-2015-309638.
11. ETH Zurich Research Collection. Altitude-adaptive model for pediatric oxygen saturation. (2019). doi:10.3929/ethz-b-000344084.
12. Floyd J, Wu L, Hay Burgess D, Izadnegahdar R, Mukanga D, Ghani AC. Evaluating the impact of pulse oximetry on childhood pneumonia mortality in resource-poor settings. *Nature* 528: S53–S59, 2015. doi:10.1038/nature16043.
13. Fouzas S, Pfitis KN, Anthracopoulos MB. Pulse oximetry in pediatric practice. *Pediatrics* 128: 740–752, 2011. doi:10.1542/peds.2011-0271.
14. Gutierrez JA, Theodorou AA. Oxygen Delivery and Oxygen Consumption in Pediatric Critical Care, in *Pediatric Critical Care Study Guide* (Lucking SE, Maffei FA, Tamburro RF, editors). Thomas, NJ: Springer, p. 19–38.
15. Habre W, Peták F. Perioperative use of oxygen: variabilities across age. *Br J Anaesth* 113, Suppl 2: ii26–ii36, 2014. doi:10.1093/bja/aeu380.
16. Harris PA, Taylor R, Thielke R, Payne J, Gonzalez N, Conde JG. Research electronic data capture (REDCap)—a metadata-driven methodology and workflow process for providing translational research informatics support. *J Biomed Inform* 42: 377–381, 2009. doi:10.1016/j.jbi.2008.08.010.
17. Hartinger SM, Lanata CF, Hattendorf J, Gil AI, Verastegui H, Ochoa T, Mäusezahl D. A community randomised controlled trial evaluating a home-based environmental intervention package of improved stoves, solar water disinfection and kitchen sinks in rural Peru: rationale, trial design and baseline findings. *Contemp Clin Trials* 32: 864–873, 2011. doi:10.1016/j.cct.2011.06.006.
18. Hartinger SM, Lanata CF, Hattendorf J, Verastegui H, Gil AI, Wolf J, Mäusezahl D. Improving household air, drinking water and hygiene in rural Peru: a community-randomized-controlled trial of an integrated environmental home-based intervention package to improve child health. *Int J Epidemiol* 45: 2089–2099, 2016. doi:10.1093/ije/dyw242.
19. Hartinger SM, Nuno N, Hattendorf J, Verastegui H, Ortiz M, Mäusezahl D, Nuño N, Verastegui H, Ortiz M, Mäusezahl D. A factorial randomised controlled trial to combine early child development and environmental interventions to reduce the negative effects of poverty on child health and development: rationale, trial design and baseline findings. *bioRxiv*, 2018. doi:10.1101/465856.
20. Hudson J, Nguku SM, Sleiman J, Karlen W, Dumont GA, Petersen CL, Warriner CB, Ansermino JM. Usability testing of a prototype Phone Oximeter with healthcare providers in high- and low-medical resource environments. *Anaesthesia* 67: 957–967, 2012. doi:10.1111/j.1365-2044.2012.07196.x.
21. International Standard Organisation. ISO 80601–2–61 Medical Electrical Equipment — Part 2–61: Particular Requirements for Basic Safety and Essential Performance of Pulse Oximeter Equipment. Geneva, ISO: 2011.
22. Karlen W, Gan H, Chiu M, Dunsmuir D, Zhou G, Dumont GA, Ansermino JM. Improving the accuracy and efficiency of respiratory rate measurements in children using mobile devices. *PLoS One* 9: e99266, 2014 [Erratum in *PLoS One* 10:e0118260, 2015]. doi:10.1371/journal.pone.0099266.
23. Karlen W, Kobayashi K, Ansermino JM, Dumont GA. Photoplethysmogram signal quality estimation using repeated Gaussian filters and cross-correlation. *Physiol Meas* 33: 1617–1629, 2012. doi:10.1088/0967-3334/33/10/1617.
24. Karlen W, Petersen CL, Dumont GA, Ansermino JM. Variability in estimating shunt from single pulse oximetry measurements. *Physiol Meas* 36: 967–981, 2015 [Erratum in *Physiol Meas* 38: 1746–1747, 2017]. doi:10.1088/0967-3334/36/5/967.
25. Karlen W, Petersen CL, Dumont GA, Ansermino JM. Corrigendum: variability in estimating shunt from single pulse oximetry measurements. *Physiol Meas* 38: 1746–1747, 2017. doi:10.1088/1361-6579/aa7c81.
26. Kasper D, Fauci AS, Hauser SL, Longo DL, Jameson JL, Loscalzo J, editors. *Harrison's Principles of Internal Medicine* (19th ed.). New York, USA: McGraw-Hill Education, 2015.
27. Luks AM, Swenson ER. Pulse oximetry at high altitude. *High Alt Med Biol* 12: 109–119, 2011. doi:10.1089/ham.2011.0013.
28. Madden K, Khemani RG, Newth CJL. Paediatric applied respiratory physiology – the essentials. *Paediatr Child Health (Oxford)* 19: 249–256, 2009. doi:10.1016/j.paed.2009.03.008.
29. Malaria Consortium. The Pneumonia Diagnostics Project: evaluating devices for accuracy [Online]. 2016. <https://www.malariaconsortium.org/resources/publications/739/The-Pneumonia-Diagnostics-Project-evaluating-devices-for-accuracy-> [5 Jun. 2019].
30. Marcante KJ, Kliegman RM, editors. *NELSON Essentials of Pediatrics* (7th ed.). Philadelphia: Elsevier Saunders, 2015.
31. Marino PL, editor. *The ICU Book* (4th ed.). Philadelphia: Lippincott Williams & Wilkins, 2013.
32. de Meer K, Heymans HSA, Zijlstra WG. Physical adaptation of children to life at high altitude. *Eur J Pediatr* 154: 263–272, 1995. doi:10.1007/BF01957359.
33. Nelson NM, Prodhom LS, Cherry RB, Smith CA. A further extension of the in vivo oxygen-dissociation curve for the blood of the newborn infant. *J Clin Invest* 43: 606–610, 1964. doi:10.1172/JCI104945.
34. Petersen CL, Gorges M, Dunsmuir D, Ansermino M, Dumont GA. Experience report: functional programming of mHealth applications. In: *Proceedings of the 18th ACM SIGPLAN International Conference on Functional Programming*. Boston: ACM Press, 2013, p. 357–362.
35. Rahn H, Otis AB. Man's respiratory response during and after acclimatization to high altitude. *Am J Physiol* 157: 445–462, 1949. doi:10.1152/ajplegacy.1949.157.3.445.
36. Rojas-Camayo J, Mejia CR, Callacondo D, Dawson JA, Posso M, Galvan CA, Davila-Arango N, Bravo EA, Loescher VY, Padilla-Deza MM, Rojas-Valero N, Velasquez-Chavez G, Clemente J, Alva-Lozada G, Quispe-Mauricio A, Bardalez S, Subhi R. Reference values for oxygen saturation from sea level to the highest human habitation in the Andes in acclimatized persons. *Thorax* 73: 776–778, 2018.
37. Schlaudecker EP, Steinhoff MC, Moore SR. Interactions of diarrhea, pneumonia, and malnutrition in childhood: recent evidence from developing countries. *Curr Opin Infect Dis* 24: 496–502, 2011. doi:10.1097/QCO.0b013e328349287d.
38. Severinghaus JW. Simple, accurate equations for human blood O<sub>2</sub> dissociation computations. *J Appl Physiol* 46: 599–602, 1979. doi:10.1152/jappl.1979.46.3.599.
39. Singh V, Aneja S. Pneumonia-management in the developing world. *Paediatr Respir Rev* 12: 52–59, 2011. doi:10.1016/j.prrv.2010.09.011.
40. Subhi R, Smith K, Duke T. When should oxygen be given to children at high altitude? A systematic review to define altitude-specific hypoxaemia. *Arch Dis Child* 94: 6–10, 2009. doi:10.1136/adc.2008.138362.
41. United Nations Children's Fund (UNICEF). *Pneumonia and Diarrhoea: Tackling The Deadliest Diseases for the World's Poorest Children*. New York: United Nations Children's Fund (UNICEF), 2012.

42. **Vargas MH, Heyaime-Lalane J, Pérez-Rodríguez L, Zúñiga-Vázquez G, Furuya MEY.** Day-night fluctuation of pulse oximetry: an exploratory study in pediatric inpatients. *Rev Invest Clin* 60: 303–310, 2008.
43. **West JB.** *Respiratory Physiology: the essential* (9th ed.). Baltimore, MD: Lippincott Williams & Wilkins, 2012.
44. **World Health Organization.** Pocket Book of Hospital Care for Children: Second Edition Guidelines for the Management of Common Childhood Illnesses. Geneva: World Health Organization, 2013.
45. **World Health Organization, The United Nations Children's Fund (UNICEF).** Ending Preventable Child Deaths from Pneumonia and Diarrhoea by 2025: The integrated Global Action Plan for Pneumonia and Diarrhoea (GAPPD). Geneva: World Health Organization/The United Nations Children's Fund (UNICEF), 2013.
46. **Yadav A.** Respiratory Monitoring. In: *Short Textbook of Anesthesia* (6th ed). New Delhi, India: Jaypee Brothers Medical Publishing, p. 61–65, 2018.

